Slope Transforms: Theory and Application to Nonlinear Signal Processing

Petros Maragos, *Senior Member, IEEE*

***Abstract*—Fourier transforms are among the most useful linear signal transformations for quantifying the frequency content of signals and for analyzing their processing by linear time-invariant systems. In this paper, some nonlinear signal transforms are developed that can provide information about the slope content of signals and are useful analytic tools for large classes of nonlinear systems. Many of their theoretical properties are examined, showing a striking conceptual resemblance to Fourier transforms and their application to linear systems. These novel transforms, called slope transforms, are originally derived from the eigenvalues of morphological dilation and erosion systems, where the corresponding eigenfunctions are lines $\alpha t + b$ parameterized by their slope α. They obey a nonlinear superposition principle of the supremum- or infimum-of-sums type. Applied to the impulse response of dilation or erosion systems, the slope transforms provide a slope response function for these systems, which allows their analysis and design in a transform domain, the slope domain. Applied to arbitrary signals, the slope transforms provide information about upper or lower tangents to the signal's graph at varying slopes. The upper or lower envelopes of the signal can be obtained from the inverse transforms. Overall, the slope transforms provide a new transform domain for signals and morphological systems where time lines become slope impulses, time cones become slope bandpass filters, and time dilation/erosion transform into addition of slope transforms. Their application to the design of slope-selective filters is also presented.**

I. Introduction

FOURIER transforms are one of the major analytic tools for quantifying the frequency content of signals. Further, they enable the analysis and design of linear time-invariant (LTI) systems in the frequency domain. For example, they transform the system's input–output description through a convolution in the time domain to the simpler operation of multiplication of transforms. Similarly, they transform the linear differential equation describing a system's time dynamics to the frequency response (a rational function of the frequency variable), which is an algebraic description of the system.

Morphological systems is a broad class of nonlinear signal operators that have found many applications in image analysis and nonlinear filtering [10], [8]. They are all based on parallel or serial interconnections of morphological dilations $\oplus$ or morphological erosions $\ominus$, defined as

$$x(t) \oplus g(t) \triangleq \bigvee_{\tau \in \boldsymbol{R}} x(\tau) + g(t-\tau) \tag{1}$$

$$x(t) \ominus g(t) \triangleq \bigwedge_{\tau \in \boldsymbol{R}} x(\tau) - g(\tau - t) \tag{2}$$

where $\bigvee$ denotes supremum and $\bigwedge$ denotes infimum. In spite of their wide applicability, so far their analysis has been done only in the time/spatial domain because of lack of transforms to describe them in a transform domain.

In this paper, we develop and study three types of nonlinear signal transforms that can quantify the slope content of signals and provide a transform domain for morphological systems; we call them *slope transforms* because they are based on eigenfunctions of morphological systems that are lines parameterized by their slope. The three types are i) a single-valued slope transform for signals processed by dilation systems, ii) a single-valued slope transform for signals processed by erosion systems, and iii) a multivalued transform that results by replacing the suprema and infima of signals with the signal values at stationary points. In the area of morphological systems and signal analysis, both transforms i) and ii) were introduced by Maragos in [7]. The contributions in this paper include the analysis of the fundamental ideas behind these transforms, their properties, and applications to morphological systems. Transform iii) was introduced by Dorst and Boomgaard [4], and part of the contributions in this paper is the study of the interrelationships among the three transforms and their relative merits. For continuous-time signals that are convex or concave and have an invertible derivative, if we ignore possible differences due to boundary effects, all three transforms coincide and become equal to the Legendre transform [3]. For discrete-time signals, only transforms i) and ii) can be used directly. Throughout the paper, we emphasize both the differences and the often striking conceptual similarities between the slope transforms and their application to nonlinear systems versus the Fourier transforms and their application to linear systems.

Ideas related to slope transforms have also appeared in other areas. For example, the Legendre transform has found numerous applications in various methods of mathematical physics [2], [3]. Further, in convex analysis [9] and optimization [1], given a convex function f, there is another useful convex function $f^\star(\alpha) = \bigvee_t \alpha t - f(t)$, called the *conjugate* of f, which is closely related to the slope transforms. Certain operations among two convex functions f, g correspond

Manuscript received December 1993; revised September 1994. This research was supported by the National Science Foundation under Grant MIP-86-58150 and under Grant MIP-93963091. The associate editor coordinating the review of this paper and approving it for publication was Dr. Thomas F. Quatieri, Jr.

P. Maragos is with the School of Electrical and Computer Engineering, Georgia Institute of Technology, Atlanta, GA 30332 USA.

IEEE Log Number 9409767.

to simpler operations among their conjugates [1], [9], e.g., $(f\square g)^\star = f^\star + g^\star$, where

$$f(t)\square g(t) \triangleq \bigwedge_\tau f(\tau) + g(t-\tau) \tag{3}$$

is called the *infimal convolution* of f and g and is closely related to erosion. Finally, in [5], planar polygonal shapes are characterized by a "slope diagram," and this representation is used to compute set dilation of these shapes.

We begin in Section II by showing that the eigenfunctions of dilation and erosion systems are lines, which leads to introducing a slope response for these systems. Section III contains the basic definitions of the three slope transforms. Sections IV and V contain many of their examples and properties. We also study in Section VI the application of slope transforms to the analysis and design of slope-selective filters and some max–min (nonlinear) differential equations that can realize them. Our work in this paper deals with continuous-time 1–D signals and systems. For completeness, however, in Section VII, we include a brief discussion on extensions of slope transforms to i) 2–D signals and ii) discrete-time signals.

II. Eigenfunctions and Slope Response of Morphological Systems

An LTI system is described either by a convolution in time or by its frequency response, which consists of the eigenvalues corresponding to the system's exponential eigenfunctions. Similarly, we show next that nonlinear systems obeying morphological-type superposition principles correspond to a morphological dilation or erosion in time and have as eigenfunctions the affine signals $\alpha t+b$, which endows them with a slope response. We begin with a brief summary of concepts behind LTI systems to see the analogies with the morphological systems.

A. Linear Time-Invariant (LTI) Systems

An LTI system is defined as a signal operator $\mathcal{L}$, mapping an input signal $x(t)$ to an output $\mathcal{L}[x(t)]$, which obeys the linear superposition principle $\mathcal{L}[\Sigma_i a_i x_i(t)] = \Sigma_i a_i \mathcal{L}[x_i(t)]$ and is time-invariant, i.e., $\mathcal{L}[x(t-t_0)] = [\mathcal{L}(x)](t-t_0)$, where $\{x_i\}$ is a finite collection of signals, t_0 is an arbitrary time shift, and a_i are real or complex weights. The output from $\mathcal{L}$ can be found via the convolution

$$\mathcal{L}[x(t)] = \int_{-\infty}^{\infty} x(\tau)h(t-\tau)\,d\tau \tag{4}$$

of the input and the impulse response $h(t)$, which is the system's output due to a Dirac delta input. The exponential signals $\exp(j\omega t)$ are eigenfunctions of $\mathcal{L}$ because

$$\mathcal{L}[\exp(j\omega t)] = H(\omega)\exp(j\omega t). \tag{5}$$

The eigenvalue $H(\omega)$, called the system's frequency response, is the Fourier transform of $h(t)$

$$H(\omega) = \int_{-\infty}^{\infty} h(t)\exp(-j\omega t)\,dt. \tag{6}$$

B. Dilation Translation-Invariant (DTI) Systems

A signal operator $\mathcal{D}{:}x \mapsto y = \mathcal{D}(x)$ is called a *dilation translation-invariant (DTI)* system if it is a lattice dilation [11], [6], i.e., if (it distributes over the supremum of any collection $\{x_i\}$ of input signals) $\mathcal{D}(\vee_i x_i) = \vee_i \mathcal{D}(x_i)$ and if it is translation-invariant, i.e., $\mathcal{D}[x(t-t_0)+c] = c+[\mathcal{D}(x)](t-t_0)$ for any real constants t_0, c. Equivalently, a system is DTI if it is time-invariant and obeys the morphological *supremum-of-sums superposition* principle

$$\mathcal{D}\left[\bigvee_i c_i + x_i(t)\right] = \bigvee_i c_i + \mathcal{D}[x_i(t)]. \tag{7}$$

Any morphological dilation (1) is a DTI system. Proving the converse requires an elementary signal, the morphological *zero impulse*

$$\mu(t) \triangleq \begin{cases} 0, & t = 0 \\ -\infty, & t \neq 0 \end{cases} \tag{8}$$

and the output of $\mathcal{D}$ when the input is this impulse, herein defined as its *impulse response* $g(t) = \mathcal{D}[\mu(t)]$. Since any signal can be represented as a supremum of translated impulses, i.e.

$$x(t) = \bigvee_{\tau=-\infty}^{\infty} x(\tau) + \mu(t-\tau) \tag{9}$$

a system is DTI if and only if its output signal is the morphological dilation of the input by its impulse response

$$\mathcal{D} \text{ is DTI } \Leftrightarrow \mathcal{D}(x) = x \oplus g, \quad g \triangleq \mathcal{D}(\mu). \tag{10}$$

Thus, in analogy to the unique description of an LTI system as a convolution by its impulse response, DTI systems are also uniquely described by a morphological dilation by their impulse response. The difference is that the integration and multiplication in the convolution are replaced by a supremum and addition in the dilation. Similarly, the summation and multiplicative weights in the linear superposition obeyed by LTI systems are replaced by a signal supremum and additive weights in the morphological superposition obeyed by DTI systems. Another subtle difference is that the useful information in a signal $x(t)$ analyzed by a DTI system exists only at times where $x(t) > -\infty$ because $-\infty$ values are ignored by the supremum in the morphological dilation. Thus, for DTI systems, the range of all signals are subsets of $\overline{\boldsymbol{R}} = \boldsymbol{R} \cup \{-\infty, \infty\}$, and the *support* of any signal $x(t)$ is defined by $\mathrm{Spt}_\vee(x) = \{t \in \boldsymbol{R} : x(t) > -\infty\}$. In contrast, the support of signals analyzed by LTI systems is the set of time instants where the signal is not zero.

The lines, i.e., affine signals $x(t) = \alpha t+b$ are *eigenfunctions* of any DTI system $\mathcal{D}$ because

$$\mathcal{D}[\alpha t + b] = \bigvee_\tau \alpha(t-\tau) + b + g(\tau) = \alpha t + b + G(\alpha) \tag{11}$$

where the corresponding eigenvalue is

$$G(\alpha) = \bigvee_t g(t) - \alpha t. \tag{12}$$

We call $G(\alpha)$ the *slope response* of the DTI system; it measures the amount of shift in the intercept of the input

lines. While the frequency response $H(\omega)$ of an LTI system is a multiplicative eigenvalue for exponential eigenfunctions $\exp(j\omega t)$, the slope response $G(\alpha)$ of a DTI system is an additive eigenvalue for affine eigenfunctions αt. Comparing (6) and (12), we also see that the frequency response of an LTI system is obtained by multiplying its impulse response by eigenfunctions $\exp(-j\omega t)$ and integrating the product, whereas the slope response of a DTI system involves adding its impulse response with eigenfunctions $-\alpha t$ and finding the supremum of the sum. Later, viewing $G(\alpha)$ as a transform for $g(t)$ will lead us to the slope transforms.

C. Erosion Translation-Invariant (ETI) Systems

The morphological erosion is a dual operation of the dilation with respect to signal negation. Hence, all the previous concepts and results for dilation systems easily extend to erosion systems with only a few changes. A signal operator $\mathcal{E} : x \mapsto y = \mathcal{E}(x)$ is called an *erosion translation-invariant (ETI)* system if it is a lattice erosion [11], [6], i.e., distributes over any infimum of input signals, and is translation-invariant. Equivalently, $\mathcal{E}$ is an ETI system if it is time-invariant and obeys the morphological *infimum-of-sums superposition* principle

$$\mathcal{E}\left[\bigwedge_i c_i + x_i(t)\right] = \bigwedge_i c_i + \mathcal{E}[x_i(t)]. \tag{13}$$

For ETI systems, a signal $x(t)$ may assume its values in $\overline{\boldsymbol{R}}$, and its support is now the set $\mathrm{Spt}_\wedge(x) = \{t \in \boldsymbol{R} : x(t) < \infty\}$. The *impulse response* of an ETI system is defined by $f(t) = \mathcal{E}[-\mu(t)]$. Since any signal can be represented as infimum of translated negated impulses, i.e.

$$x(t) = \bigwedge_{\tau=-\infty}^{\infty} x(\tau) - \mu(t-\tau) \tag{14}$$

a system is ETI if and only if its output is the infimal convolution of the input with the impulse response

$$\mathcal{E} \text{ is ETI } \Leftrightarrow \mathcal{E}(x) = x \square f, \qquad f \triangleq \mathcal{E}(-\mu). \tag{15}$$

Note that $x(t)\square f(t) = x(t) \ominus (-f(-t))$; hence, the output of an ETI system is the morphological erosion of the input by the negated and reflected impulse response.

The affine signals $x(t) = \alpha t + b$ are *eigenfunctions* of any ETI system $\mathcal{E}$ because

$$\mathcal{E}[\alpha t + b] = \alpha t + b + F(\alpha) \tag{16}$$

with corresponding eigenvalue

$$F(\alpha) = \bigwedge_t f(t) - \alpha t. \tag{17}$$

We shall call $F(\alpha)$ the *slope response* of the ETI system.

III. Slope Transforms

To acquire a geometrical intuition behind the slope transforms, we precede their definitions with a brief summary of concepts from the related Legendre transform and some definitions of concave and convex signals for which the analysis of slope transforms is simple.

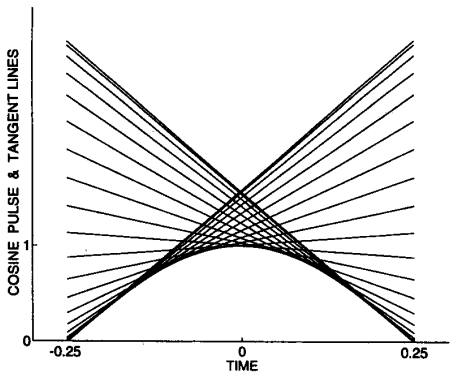

Fig. 1. Concave signal ($\cos(2\pi t)$, $|t| \le 0.25$) as the lower envelope of its tangent lines.

A. Convex and Concave Signals

Given a function $f : \boldsymbol{R} \to \boldsymbol{R}$, f is *concave* if and only if

$$f(t) \ge \frac{pf(t-q) + qf(t+p)}{p+q} \quad \forall p, q > 0 \text{ and } \forall t. \tag{18}$$

For equivalent definitions, see [9]. If its domain is smaller than $\boldsymbol{R}$, the function f can be viewed as concave over all $\boldsymbol{R}$ by allowing it to have $-\infty$ values at all points where it was originally undefined [9]. A concave function is called *proper* if $f(t) > -\infty$ for at least one t and $f(t) < +\infty$ for all t. A function f is *convex* if $-f$ is concave. Henceforth, whenever we talk about concave or convex functions, we shall assume they are proper, unless otherwise stated.

B. Legendre Transform

Let the signal $x(t)$ be concave and have an invertible derivative $x' = dx/dt$. The Legendre transform of x is based on the concept of imagining the graph of x, not as a set of points $(t, x(t))$ but as the lower envelope of all its tangent lines; e.g., see Fig. 1. The tangent at a point $(t, x(t))$ on the graph has *slope*

$$\alpha = x'(t) \tag{19}$$

and *intercept* equal to

$$X = x(t) - \alpha t. \tag{20}$$

Using (19) to eliminate t from (20) makes the intercept

$$X_L(\alpha) = x((x')^{-1}(\alpha)) - \alpha[(x')^{-1}(\alpha)] \tag{21}$$

where f^{-1} denotes the inverse of a function f. The function X_L of the tangent's intercept versus the slope is the Legendre transform [2] of x. For an inverse transform note that by (20)

$$X'(\alpha) = -t. \tag{22}$$

Using this equation to eliminate α from (20) yields the signal x from its Legendre transform

$$x(t) = X_L((X_L')^{-1}(-t)) + t[(X_L')^{-1}(-t)]. \tag{23}$$

The right-hand side is the inverse Legendre transform of X_L.

If the signal x is convex, then the signal is viewed as the upper envelope of its tangent lines. Although in the classical literature the Legendre transform is defined only for convex functions, its definition in (21) makes sense both for convex and concave signals. If the signal derivative is not invertible or the signal is not everywhere differentiable or if the signal is neither convex nor concave, there are more general transforms discussed next.

C. Slope Transform Based on Supremum

Viewing the slope response (12) as a signal transform with variable the slope α, Maragos [7] was motivated to define for any signal $x : \boldsymbol{R} \to \overline{\boldsymbol{R}}$ its *upper slope transform* as the function $X_\vee : \boldsymbol{R} \to \overline{\boldsymbol{R}}$ with

$$X_\vee(\alpha) \triangleq \bigvee_{t \in \boldsymbol{R}} x(t) - \alpha t, \quad \alpha \in \boldsymbol{R}. \tag{24}$$

The mapping between the signal and its transform is denoted by $\mathcal{A}_\vee : x \mapsto X_\vee$. If there is one-to-one correspondence between the signal and its transform, we may write this as $x(t) \overset{\mathcal{A}_\vee}{\longleftrightarrow} X_\vee(\alpha)$. The subscript $\vee$ in X is to differentiate this transform from another that is based on infimum, and it will occasionally be dropped if understood from the context.

The definition (24) was motivated by the form of the eigenfunctions and eigenvalues of DTI systems. However, there is also a close relationship with the Legendre transform. To see this, assume that the signal $x(t)$ is concave and has an invertible derivative. For each real α, the *intercept* of the line passing from the point $(t, x(t))$ on the signal's graph with slope α is equal to $x(t) - \alpha t$ (see Fig. 2). For a fixed α, as t varies there is a time instant t^* for which the intercept attains its maximum value. This occurs when the line becomes *tangent* to the graph; then we have $x'(t^*) = \alpha$. As α varies, the tangent changes, and the maximum intercept becomes a function of the slope α. By its definition, the upper slope transform is equal to this maximum intercept function. Further, the maximization of the concave function $x(t) - \alpha t$ can be found from its value at its unique stationary point t^* where $x'(t^*) = \alpha$. Thus, if the signal x is concave and has an invertible derivative, then the upper slope transform is equal to its Legendre transform (with possible exception over slope intervals controlled by the signal's boundaries). For such an example, consider the concave cosine pulse

$$y(t) = \begin{cases} \cos(\omega_0 t), & |t| \le T/4 \\ -\infty, & |t| > T/4 \end{cases}; \quad T = \frac{2\pi}{\omega_0}. \tag{25}$$

For $|t| \le T/4, y'(t) = -\omega_0 \sin(\omega_0 t) = \alpha$ and the maximum intercept occurs at $t^* = -\arcsin(\alpha/\omega_0)/\omega_0$, where $|\alpha| \le \omega_0$ and $|\arcsin()| \le \pi/2$. Thus

$$Y_\vee(\alpha) = \begin{cases} \sqrt{1 - \dfrac{\alpha^2}{\omega_0^2}} + \left(\dfrac{\alpha}{\omega_0}\right) \arcsin\left(\dfrac{\alpha}{\omega_0}\right), & |\alpha| \le \omega_0 \\ T|\alpha|/4, & |\alpha| > \omega_0. \end{cases} \tag{26}$$

Note that for $|\alpha| > \omega_0$, the Legendre transform is not defined, but the upper slope transform consists of lines $T|\alpha|/4$ due to the signal boundaries over $|t| > T/4$.

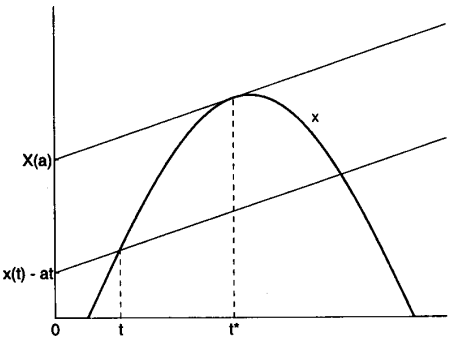

Fig. 2. Concave signal x, its tangent with slope α, and a line parallel to the tangent.

Now, if the signal is concave but either i) it does not have an invertible derivative, e.g., when its graph contains some line segments, or ii) it is not differentiable everywhere on its support, e.g., when it has some corner points, then its Legendre transform is not well (or cannot be) defined, but the upper slope transform still gives an answer. An important example of case i) is the signal $x(t) = \alpha_0 t + b$. Then x' is not invertible, but the maximization of the intercept becomes simple if we express it via the supremum in (24). Thus, $X_\vee(\alpha) = b + \bigvee_t (\alpha_0 - \alpha)t$, which yields

$$\alpha_0 t + b \overset{\mathcal{A}_\vee}{\longleftrightarrow} b - \mu(\alpha - \alpha_0) = \begin{cases} b, & \alpha = \alpha_0 \\ +\infty, & \alpha \ne \alpha_0. \end{cases} \tag{27}$$

Thus, as the Fourier transform of an LTI system's eigenfunction $\exp(j\omega_0 t)$ is a Dirac impulse at frequency ω_0, the upper slope transform of a DTI system's eigenfunction $\alpha_0 t + b$ is a morphological impulse at slope α_0.

If the signal is neither concave nor convex, then its Legendre transform is not a single-valued function. In this case, the upper slope transform still provides a single-valued function, which is the slope transform of the upper concave envelope of the signal, as explained next.

In general

$$x(t) \le X_\vee(\alpha) + \alpha t, \forall \alpha, \forall t. \tag{28}$$

Thus, $x(t)$ is covered from above by all the lines $X_\vee(\alpha) + \alpha t$, and hence, $x(t) \le \hat{x}(t)$ where

$$\hat{x}(t) \triangleq \bigwedge_{\alpha \in \boldsymbol{R}} X_\vee(\alpha) + \alpha t. \tag{29}$$

We view the mapping $X_\vee \mapsto \hat{x}$ as an *'inverse' upper slope transform* of $X_\vee$, which yields a signal $\hat{x}$ that is sometimes equal to x and never smaller. Further, at any time instant t, we shall show that the reconstructed signal value $\hat{x}(t)$ is equal to the original $x(t)$ if and only if

$$x(t) \ge \frac{px(t-q) + qx(t+p)}{p+q} \qquad \forall p, q > 0 \tag{30}$$

assuming[1] $x(v) < +\infty$ for all v. We can view (30) as a definition of a "pointwise concavity": A signal $x(t)$ is called

[1]The assumption $x(v) < +\infty \, \forall v$ helps avoiding undefined cases such as $-\infty + \infty$.

pointwise concave at a point t if it satisfies (30). An alternative way to interpret (30) is for any point $A = (t-q, x(t-q))$ on the signal's graph to the left of $B = (t, x(t))$ and for any point $C = (t+p, x(t+p))$ to its right, the slope of the left segment $\overline{AB}$ is not smaller than the slope of the right segment $\overline{BC}$. Of course, a signal is concave if it is pointwise concave at all the points of its domain.

The following theorem states several important properties of the upper slope transform and its inverse.

Theorem 1: For any[2] signal $x : \boldsymbol{R} \to \boldsymbol{R} \cup \{-\infty\}$, the following hold:

a) $X_\vee$ is convex and $\hat{x}$ is concave.
b) For all t, $\hat{x}(t) \geq x(t)$.
c) At any time instant $t, \hat{x}(t) = x(t)$ if and only if $x(t)$ satisfies (30).
d) $\hat{x}(t) = x(t)$ for all t if x is concave and upper semicontinuous.
e) $\hat{x}$ is the smallest concave upper envelope of x.

Proof: We denote $X_\vee$ simply by X.

a) is true because $X(\alpha)$ is the supremum of the lines $x(t)-\alpha t$ and $\hat{x}(t)$ is the infimum of the lines $X(\alpha)+\alpha t$.
b) follows from (28).
c) Sufficiency: At some time t, let $x(t)$ satisfy (30), which can be rewritten as

$$\frac{x(t+p)-x(t)}{p} \leq \frac{x(t)-x(t-q)}{q} \qquad \forall p, q > 0. \quad (31)$$

This is equivalent to saying there exists $\alpha_0 \in \boldsymbol{R}$ such that

$$\frac{x(t+p)-x(t)}{p} \leq \alpha_0 \leq \frac{x(t)-x(t-q)}{q} \qquad \forall p, q > 0 \quad (32)$$

or equivalently that

$$\exists \alpha_0 \text{ s.t. } x(t) - \alpha_0 t \geq x(\tau) - \alpha_0 \tau \qquad \forall \tau \neq t. \quad (33)$$

Then $X(\alpha_0) = x(t) - \alpha_0 t$ and hence, $x(t) = X(\alpha_0) + \alpha_0 t$. This implies that $x(t) \geq \hat{x}(t)$, which coupled with (b) proves that $x(t) = \hat{x}(t)$ if (30) is true. Necessity: Assume now $x(t) = \hat{x}(t)$. Then, for all $p, q > 0$

$$\begin{aligned}\frac{px(t-q)+qx(t+p)}{p+q} &= \frac{p\bigwedge_\alpha X(\alpha)+\alpha(t-q)+q\bigwedge_\alpha X(\alpha)+\alpha(t+p)}{p+q} \\ &\leq \frac{\bigwedge_\alpha (p+q)X(\alpha)+\alpha t(p+q)}{p+q} = x(t).\end{aligned}$$

Thus, (30) is true if $x(t) = \hat{x}(t)$, and the proof of (c) is complete.
d) results from (c) and (18). Note: Since x is concave, it is upper semicontinuous in the interior of its support. Upper semicontinuity is needed only to guarantee closure at boundary points. From a different viewpoint, assuming the concave x is proper, upper semicontinuity is equivalent to x being "closed" [9]. (Note that $\hat{x}$ is always closed.)
e) Since $\hat{x} \geq x, \hat{x}$ is an upper concave envelope of x. Assume now that there is another signal y that is an upper concave envelope of x but smaller than $\hat{x}$, i.e., $x(t) \leq y(t) \leq \hat{x}(t)$ for all t. Then $\mathcal{A}_\vee(x) \leq \mathcal{A}_\vee(y) \leq \mathcal{A}_\vee(\hat{x}) = \mathcal{A}_\vee(x)$. Hence, $\mathcal{A}_\vee(y) = \mathcal{A}_\vee(\hat{x})$. Since now the mapping $\mathcal{A}_\vee$ is one-to-one on concave signals, we obtain $y = \hat{x}$, which completes the proof. Q.E.D.

Thus, there is one-to-one correspondence between $X_\vee$ and the signal envelope $\hat{x}$. Of course, x will be exactly reconstructed via $\hat{x}$ if x is concave. Otherwise, all signals between x and $\hat{x}$ will have the same slope transform

$$x(t) \leq y(t) \leq \hat{x}(t)\ \forall t \Rightarrow X_\vee(\alpha) = Y_\vee(\alpha)\ \forall \alpha. \quad (34)$$

Let a signal x be concave and have an invertible derivative. Then its Legendre transform X is equal to its upper slope transform, ignoring possible boundary effects. Since x is the lower envelope of all its tangents, for each t we can reconstruct $x(t)$ by finding the minimum value of $X(\alpha) + \alpha t$. This minimum is the value of the inverse upper slope transform. Further, since X is convex and has an invertible derivative, this minimum value will occur at a unique slope α^* such that $X'(\alpha^*) = -t$. Thus, in this case, the inverse Legendre transform and the inverse upper slope transform will yield identical results. For such an example, consider the cosine pulse $y(t) = \cos(\omega_0 t), |t| \leq \pi/2\omega_0$ and its Legendre transform $Y(\alpha)$ equal to the function in (26) over $|\alpha| \leq \omega_0$. Then, since $Y(\alpha)$ is convex and differentiable, the minimization over α of the convex function $Y(\alpha) + \alpha t$ can be done either by taking its global infimum or equivalently by finding its value at the stationary point $\alpha^* = (Y')^{-1}(-t) = -\omega_0 \sin(\omega_0 t)$. Thus, the inverse transform reconstructs the signal $Y(\alpha^*) + \alpha^* t = y(t)$.

As another example, consider the slope transform (27) of a line $x(t) = \alpha_0 t + b$. In this case, the transform is not differentiable. Hence, the minimization of $X(\alpha) + \alpha t$ cannot be done using stationary points. However, the inverse upper slope transform yields the answer in a simple way

$$\bigwedge_\alpha b - \mu(\alpha - \alpha_0) + \alpha t = b + \alpha_0 t.$$

D. Slope Transform Based on Infimum

The form of the eigenfunctions and eigenvalues (slope response) of ETI systems in (17) motivated us in [7] to define for any signal $x : \boldsymbol{R} \to \overline{\boldsymbol{R}}$ its *lower slope transform* as the function $X_\wedge : \boldsymbol{R} \to \overline{\boldsymbol{R}}$ with

$$X_\wedge(\alpha) \triangleq \bigwedge_{t \in \boldsymbol{R}} x(t) - \alpha t, \qquad \alpha \in \boldsymbol{R}. \quad (35)$$

Denoting the mapping between the signal and its lower slope transform by $\mathcal{A}_\wedge : x \mapsto X_\wedge$, we easily find a relationship between the upper and lower slope transform

$$\mathcal{A}_\wedge[x(t)](\alpha) = -\mathcal{A}_\vee[-x(t)](-\alpha) = -\mathcal{A}_\vee[-x(-t)](\alpha). \quad (36)$$

[2] Although we allow a signal and its slope transform to also assume $\pm\infty$ values, these extreme values usually correspond to trivial cases. For example, if $x(t) = +\infty$ for at least one t, then $X_\vee(\alpha) = +\infty\ \forall \alpha$ and $\hat{x}(t) = +\infty\ \forall t$. Also, $X_\vee(\alpha) > -\infty$ for all α unless $x(t) = -\infty\ \forall t$. If $x \equiv -\infty$, then $X_\vee \equiv -\infty$ and $\hat{x} \equiv -\infty$.

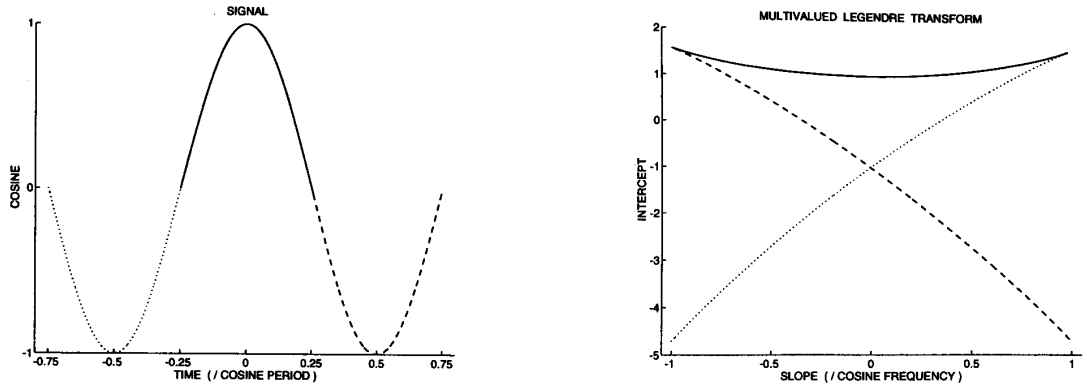

(a) (b)

Fig. 3. (a) Three half-periods of a cosine and (b) the upper or lower slope transforms (equal to Legendre transforms) of the three concave or convex cosine pulses. (Time pulses and their transforms have the same line types.)

Whatever we discussed for upper slope transforms also applies to the lower slope transform, the only differences being that the term pairs supremum/infimum and concave/convex must be interchanged. If a signal is convex and has an invertible derivative over its support, then its lower slope transform is equal to its Legendre transform (except over slope regions controlled by the signal's boundaries). Such an example is the convex cosine pulse $z(t) = -y(t)$, where y is the concave signal in (25); then $Z_\wedge(\alpha) = -Y_\vee(\alpha)$. Now, if a signal is not everywhere differentiable or does not have an invertible derivative, then the lower slope transform should be used instead of the Legendre transform. For example, if $x(t) = \alpha_0 t + b$, then $X_\wedge(\alpha) = b + \bigwedge_t(\alpha_0 - \alpha)t$, which yields

$$\alpha_0 t + b \overset{\mathcal{A}_\wedge}{\longleftrightarrow} b + \mu(\alpha - \alpha_0). \tag{37}$$

By duality to the upper slope transform, the *inverse lower slope transform* of $X_\wedge$ is the signal

$$\check{x}(t) \triangleq \bigvee_{\alpha \in \boldsymbol{R}} X_\wedge(\alpha) + \alpha t \tag{38}$$

that is sometimes equal to $x(t)$ and never larger. By working as for upper slope transforms, the following properties of the lower slope transform and its inverse can be found:

Theorem 2: For any signal $x : \boldsymbol{R} \to \boldsymbol{R} \cup \{+\infty\}$

a) $X_\wedge$ is concave, and $\check{x}$ is convex.

b) For all $t, \check{x}(t) \le x(t)$.

c) At any time instant t

$$\check{x}(t) = x(t) \Leftrightarrow x(t) \le \frac{px(t-q) + qx(t+p)}{p+q} \quad \forall p, q > 0. \tag{39}$$

d) $\check{x}(t) = x(t)$ for all t if x is convex and lower semicontinuous.

e) $\check{x}$ is the largest convex lower envelope of x.

Thus, any signal between x and $\check{x}$ will have the same lower slope transform as x, i.e.

$$x(t) \ge y(t) \ge \check{x}(t)\ \forall t \Rightarrow X_\wedge(\alpha) = Y_\wedge(\alpha)\ \forall \alpha. \tag{40}$$

The correspondence of $X_\wedge$ with the lower envelope $\check{x}$ (and with the signal x if the latter is convex) is one-to-one.

Finally we note that, given a convex function f, its conjugate $f^\star$ from convex analysis [9] is closely related to its lower slope transform since $f^\star = -F_\wedge$.

E. Slope Transform Based on Stationary Points

Dorst and Boomgaard [4] extended the Legendre transform to arbitrary differentiable signals by rewriting (21) as

$$X_{\text{stat}}(\alpha) \triangleq \{x(t) - \alpha t : x'(t) = \alpha\}. \tag{41}$$

If x' is invertible, then X_{stat} is a single-valued function identical to the Legendre transform of x given by (21). If x is differentiable but is neither convex nor concave, then X_{stat} is a multivalued function, i.e., a set collection of single-valued transform functions. Thus, for each $\alpha, X_{\text{stat}}(\alpha)$ is a set of numbers since the equation $x'(t) = \alpha$ might have more than one solutions. Obviously, the two definitions in (21) and (41) are equivalent if we interpret $(x')^{-1}(\alpha)$ more generally as the set $\mathcal{T} = \{t : x'(t) = \alpha\}$ and $x(\mathcal{T})$ as the image of $\mathcal{T}$ under x. It is this generally *multivalued Legendre transform* that was defined in [4] as a slope transform for differentiable signals.

For example, consider the signal

$$x(t) = \cos(\omega_0 t), \quad |t| \le \frac{3T}{4}, \quad T = \frac{2\pi}{\omega_0} \tag{42}$$

which is a sequence of two convex and one concave half-period cosine pulses. Then its multivalued Legendre transform (shown in Fig. 3) consists of three different functions, one for each convex or concave piece, as follows:

$$X_{\text{stat}}(\alpha) = \left\{-Y_L(\alpha) + \frac{\alpha T}{2}, Y_L(\alpha), -Y_L(\alpha) - \frac{\alpha T}{2}\right\} \tag{43}$$

where Y_L is the Legendre transform for a single cosine pulse $y(t) = \cos(\omega_0 t), |t| \le T/4$ equal to the slope transform in (26) for $|\alpha| \le \omega_0$. In general, the number of different functions in the multivalued Legendre transform is equal to the number of consecutive convex and concave pieces making up the signal.

Assuming the original signal $x(t)$ is a sequence of convex or concave pieces each possessing invertible derivatives, we can exactly reconstruct it by applying the inverse Legendre

transform to each single-valued function belonging to the multivalued transform $X_{\text{stat}}(\alpha)$. Each such usage of the inverse Legendre transform will reconstruct the original signal *only* over the time interval over which the corresponding convex or concave piece is defined. For example, in the case of the signal in (42), the inverse Legendre transform of $Y_L(\alpha)$ will reconstruct $\cos(\omega_0 t)$ only over $t \in [-T/4, T/4]$. whereas the inverse Legendre transform of $-Y_L(\alpha) - \alpha T/2$ will reconstruct $\cos(\omega_0 t)$ only over $t \in [T/4, 3T/4]$.

Finally, note that the above multivalued transform can be extended to nondifferentiable signals by replacing the Legendre transforms of each signal piece with the more general upper or lower slope transforms.

IV. Examples of Slope Transforms

Example 1: Time impulse and step: The impulse in time becomes a line in slope domain

$$\mu(t - t_0) \overset{\mathcal{A}_\vee}{\longleftrightarrow} -\alpha t_0. \tag{44}$$

Another elementary signal is the morphological *zero step*

$$\lambda(t) \triangleq \begin{cases} 0, & t \geq 0 \\ -\infty, & t < 0. \end{cases} \tag{45}$$

The slope transform of a shifted step $\lambda(t - t_0)$ is $\bigvee_{t \geq t_0} -\alpha t$, which is equal to a half-line in the slope domain

$$\lambda(t - t_0) \overset{\mathcal{A}_\vee}{\longleftrightarrow} -\alpha t_0 - \lambda(\alpha). \tag{46}$$

Example 2: Time pulse: The concave symmetric zero pulse x has as its upper slope transform a convex cone

$$x(t) = \begin{cases} 0, & |t| \leq T \\ -\infty, & |t| > T \end{cases} \overset{\mathcal{A}_\vee}{\longleftrightarrow} X_\vee(\alpha) = T|\alpha|. \tag{47}$$

By (36), the convex time pulse $y(t) = -x(t)$ transforms into a concave slope cone $Y_\wedge(\alpha) = -T|\alpha|$.

Example 3: Causal line: Consider a signal $x(t) = \alpha_0(t) + \lambda(t)$ equal to $\alpha_0 t$ for $t \geq 0$ and $-\infty$ elsewhere. Thus, adding to a signal the step $\lambda(t)$ makes it right-sided, also called "causal."[3] Since $X_\vee(\alpha) = \vee_{t \geq 0}(\alpha_0 - \alpha)t$

$$\alpha_0 t + \lambda(t) \overset{\mathcal{A}_\vee}{\longleftrightarrow} \lambda(\alpha - \alpha_0). \tag{48}$$

Thus, a causal line transforms into a negated shifted step in the slope domain. Its lower slope transform is a reflected shifted step

$$\alpha_0 t - \lambda(t) \overset{\mathcal{A}_\wedge}{\longleftrightarrow} \lambda(\alpha_0 - \alpha). \tag{49}$$

A DTI system whose impulse response is the causal line $\alpha_0 t + \lambda(t)$ behaves as a *slope highpass* filter, which suppresses all input lines with slope smaller than α_0 and leaves all higher slopes unchanged. Note that for the slope response of DTI systems a value of $+\infty$ corresponds to suppressing the corresponding slope, whereas a value of 0 leaves it unchanged. Similarly, an ETI system whose impulse response is the causal line $\alpha_0 t - \lambda(t)$ behaves as a slope lowpass filter, rejecting all slopes higher than α_0 and passing the rest.

[3]We call right-sided signals "causal," borrowing the terminology from the case where the signal is the impulse response of a causal dilation or erosion system.

Example 4: Time cone: Let $x(t) = -\alpha_0|t|, \alpha_0 > 0$ be an even concave cone. By using the duality between time and slope domains (explained in Section V), its upper slope transform is an even convex slope pulse

$$x(t) = -\alpha_0|t| \overset{\mathcal{A}_\vee}{\longleftrightarrow} X_\vee(\alpha) = \begin{cases} 0, & |\alpha| \leq \alpha_0 \\ +\infty, & |\alpha| > \alpha_0. \end{cases} \tag{50}$$

By (36), the lower slope transform of an even convex cone $y(t) = -x(t)$ is a concave slope pulse $Y_\wedge(\alpha) = -X_\vee(\alpha)$. Thus, DTI or ETI systems whose impulse responses are these conical functions behave as ideal-cutoff symmetric slope bandpass filters.

Example 5: Piecewise-linear signal: Consider a concave signal that is a piecewise-linear function $x(t)$ with corner points at the time instants $t_1 < t_2 < \cdots < t_m$ and corresponding values $x_1, x_2, \cdots, x_m$. Let $\alpha_0 \geq \alpha_1 \geq \cdots \geq \alpha_m$ be the slopes of the $m+1$ line pieces comprising the signal from left to right. The $m-1$ intermediate segments have slopes

$$\alpha_k = \frac{x_{k+1} - x_k}{t_{k+1} - t_k}, \qquad k = 1, 2, \cdots, m-1 \tag{51}$$

determined by the corner-point data. The upper slope transform of $x(t)$ is a convex piecewise-linear function

$$X_\vee(\alpha) = \begin{cases} +\infty, & \alpha > \alpha_0 \\ x_k - \alpha t_k, & \alpha_{k-1} \geq \alpha \geq \alpha_k, \\ +\infty, & \alpha < \alpha_m. \end{cases} \qquad k = 1, \cdots, m \tag{52}$$

Thus, the class of concave or convex piecewise-linear signals is mapped onto itself under the upper or lower slope transform.

The rest of the examples deal with known mathematical functions x possessing invertible derivatives. Hence, ignoring possible differences due to boundary effects, the slope transforms of their concave or convex subparts become equal to Legendre transforms, which can be found using stationary point values $x(t^*) - \alpha t^*$ where $x'(t^*) = \alpha$.

Example 6: Circle: Let $x(t) = \sqrt{1 - t^2}, |t| \leq 1$. The maximum intercept is $x(t^*) - \alpha t^*$, where $t^* = \alpha/\sqrt{1 + \alpha^2}$. Hence

$$x(t) = \begin{cases} \sqrt{1 - t^2}, & |t| \leq 1 \\ -\infty, & |t| > 1 \end{cases} \overset{\mathcal{A}_\vee}{\longleftrightarrow} X_\vee(\alpha) = \sqrt{1 + \alpha^2}. \tag{53}$$

Example 7: Parabola: Let $x(t) = -t^2/2$. Substituting $t^* = (x')^{-1}(\alpha) = -\alpha$ into $x(t^*) - \alpha t^*$ gives

$$-t^2/2 \overset{\mathcal{A}_\vee}{\longleftrightarrow} \alpha^2/2. \tag{54}$$

As observed in [4], the parabola plays the same role in slope transforms as the Gaussian function does for Fourier transforms. Further, as in the case of piecewise-linear signals, its transform belongs to the same class of functions as the signal. The parabola transform pair is actually a special case of a general class of conjugate concave/convex functions [9]

$$-|t|^p/p \overset{\mathcal{A}_\vee}{\longleftrightarrow} |\alpha|^q/q, \quad \frac{1}{p} + \frac{1}{q} = 1, \qquad p, q > 1. \tag{55}$$

Example 8: Exponential: Let $x(t) = \exp(t)$. Setting $x'(t) = \exp(t) = \alpha$ yields $t^* = \log(\alpha)$ for $\alpha > 0$. Hence

$$\exp(t) \overset{\mathcal{A}_\vee}{\longleftrightarrow} \alpha[1 - \log(\alpha)] - \lambda(\alpha). \tag{56}$$

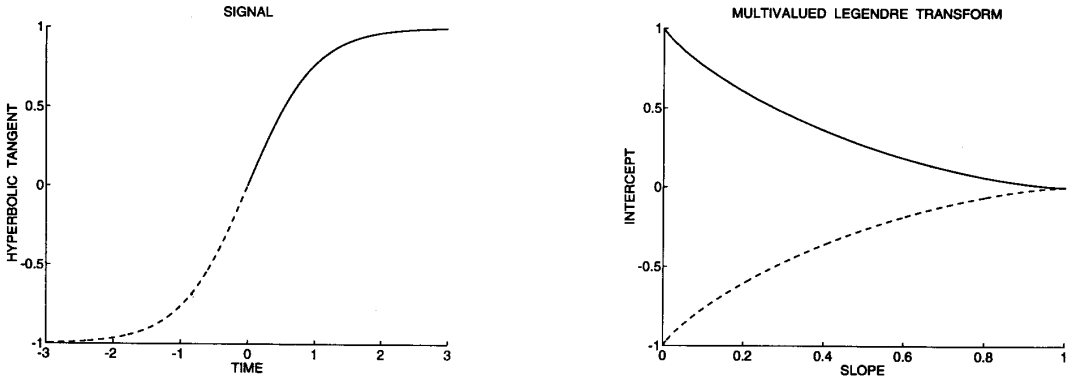

(a) (b)

Fig. 4. (a) Signal $\tanh(t)$ and (b) its two-valued slope transform. (Signal segments and their transforms have same line types.)

Example 9: Hyperbolic tangent: Let $x(t) = \tanh(t)$. Since $x'(t) = 1/\cosh^2(t)$, the slope is limited to $0 \leq \alpha \leq 1$. Then $t^* = \cosh^{-1}(1/\sqrt{\alpha})$. The signal consists of one convex piece $z(t)$ (over $t \leq 0$) and one concave piece $y(t)$ (over $t \geq 0$). The concave piece has Legendre transform

$$Y_L(\alpha) = \sqrt{1-\alpha} - \alpha \log\left(\frac{1+\sqrt{1-\alpha}}{\sqrt{\alpha}}\right), \qquad 0 \leq \alpha \leq 1. \tag{57}$$

The upper slope transform pair is $y(t) + \lambda(t) \overset{\mathcal{A}_\vee}{\longleftrightarrow} Y_L(\alpha) - \lambda(\alpha)$. For the negative-time piece, observe that $z(t) = -y(-t)$. Hence, by (36), $Z_L(\alpha) = -Y_L(\alpha)$. Thus, the two-valued Legendre transform of $\tanh(t)$ is equal to $\{Y_L(\alpha), -Y_L(\alpha)\}$. Fig. 4 shows the two signal pieces and their transforms.

Example 10: Entropy pulse: The entropy of a binary source that produces the symbols 0 and 1 with probabilities t and $1-t$ is given by $x(t) = -t\log(t) - (1-t)\log(1-t)$ with $0 \leq t \leq 1$. Assume $x(t) = -\infty$ if $t<0$ or $t>1$. Setting $x'(t) = \log[(1-t)/t] = \alpha$ yields that the maximum intercept occurs at $t^* = 1/[1+\exp(\alpha)]$ for any α. Hence

$$X_\vee(\alpha) = \log[1+\exp(\alpha)] - \alpha. \tag{58}$$

Note the differences between the upper slope and Legendre transforms due to *boundary effects*. In examples 6, 9, and 10, the Legendre transform allows the time signals to exist only over their function domains. In contrast, the upper slope transform allows the signal to be defined over the whole time axis by using $-\infty$ values for padding. Similarly, in examples 8 and 9, the Legendre transform allows the slope functions to be defined only over their initial domains, whereas the upper slope transform can always yield values over the whole slope axis.

V. Properties of Slope Transforms

Table I lists several properties of the upper slope transform. Again, we observe many similarities among properties of Fourier and slope transforms, where the general analogy appears to be as follows: Signal summation or multiplication in Fourier transforms becomes supremum or addition in slope transforms, multiplicative weights become additive, and complex exponentials become lines. Next we prove a few of these properties. The proofs of the rest can be derived easily. We shall use the notation $X(\alpha) = \bigvee_t x(t) - \alpha t$.

TABLE I
Properties of Upper Slope Transform

Signal	Transform
$x(t)$	$X(\alpha) = \bigvee_t x(t) - \alpha t$
$\bigvee_i c_i + x_i(t)$	$\bigvee_i c_i + X_i(\alpha)$
$x(t-t_0)$	$X(\alpha) - \alpha t_0$
$x(t) + \alpha_0 t$	$X(\alpha - \alpha_0)$
$x(rt)$	$X(\alpha/r)$
$x(-t)$	$X(-\alpha)$
$x(t) = x(-t)$	$X(\alpha) = X(-\alpha)$
$rx(t)$, $r>0$	$rX(\alpha/r)$
$x(t) \oplus y(t)$	$X(\alpha) + Y(\alpha)$
$\bigvee_\tau x(\tau) + y(t+\tau)$	$X(-\alpha) + Y(\alpha)$
$x(t) \leq y(t)\ \forall t$	$X(\alpha) \leq Y(\alpha)\ \forall \alpha$
$\bigvee_t x(t) = X(0)$	$\bigwedge_\alpha X(\alpha) \geq x(0)$
$x(t) \wedge y(t)$	$\leq X(\alpha) \wedge Y(\alpha)$
$x(t) + y(t)$	$\leq X(\alpha) \square Y(\alpha)$
$x(t) + y(t)$, y is convex	$X_\vee(\alpha) \oplus Y_\wedge(\alpha)$
$y(t) = \begin{cases} x(t), & \lvert t\rvert \leq T \\ -\infty, & \lvert t\rvert > T \end{cases}$	$Y(\alpha) = X(\alpha) \square T\lvert\alpha\rvert$

Time/Slope Shift: A shift of a signal in time by t_0 adds to its slope transform the line $-\alpha t_0$ because

$$x(t-t_0) \overset{\mathcal{A}_\vee}{\longleftrightarrow} \bigvee_t x(t-t_0) - \alpha t = -\alpha t_0 + X(\alpha). \tag{59}$$

For example, in Fig. 3, the first and last cosine pulses are shifted versions of the center pulse by $\pm T/2$; this adds a component of $\mp \alpha T/2$ to the slope transforms. Similarly, a shift of the transform by α_0 adds to the signal the line $\alpha_0 t$.

Signal Dilation in Time:

$$\begin{aligned} \mathcal{A}_\vee[x(t) \oplus y(t)](\alpha) &= \bigvee_t \left(\bigvee_\tau x(\tau) + y(t-\tau) \right) - \alpha t \\ &= \bigvee_\tau x(\tau) + \left(\bigvee_t y(t-\tau) - \alpha t \right) \\ &= \bigvee_\tau x(\tau) + Y(\alpha) - \alpha\tau \\ &= X(\alpha) + Y(\alpha). \end{aligned} \tag{60}$$

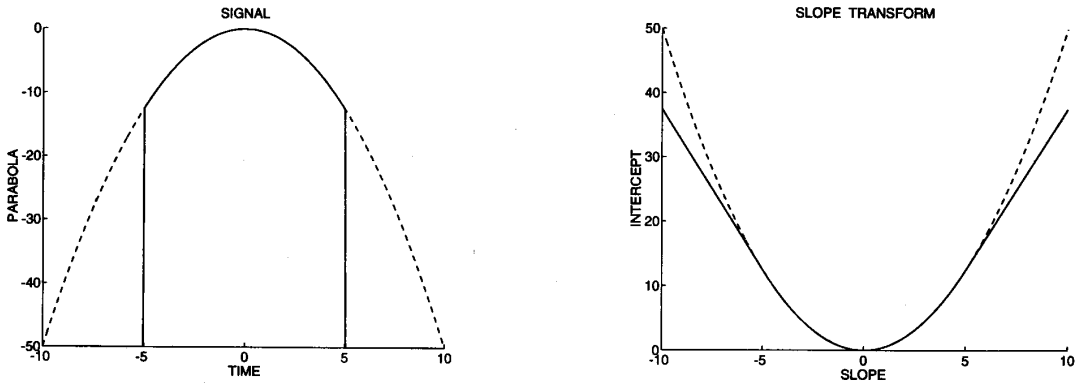

(a) (b)

Fig. 5. (a) Original parabola signal $x(t) = -t^2/2$ (in dashed line) and a time-limited version (in solid line) resulting from adding to the signal a rectangular pulse with support $[-5, 5]$. (b) Upper slope transform of the parabola (in dashed line) and of its time-limited version (in solid line).

This is the most important property: Dilation in the time domain corresponds to addition in the slope domain. If two signals are concave, then their dilation can be done by first transforming the signals to the slope domain, adding their upper slope transforms, and then returning back to the time domain via the inverse upper slope transform. This opens new ways of implementing dilations, since addition is a much simpler operation. Contrast the above idea with the correspondence between convolving two signals in the time domain and multiplying their Fourier transforms. Finally, by the above property and since time reflection causes slope reflection, the *nonlinear autocorrelation* (maximum of sums) $\bigvee_\tau x(\tau)+x(t+\tau)$ corresponds to adding $X(\alpha)$ and $X(-\alpha)$.

Signal Addition in Time: For any signals x, y

$$\begin{aligned}\mathcal{A}_\vee[x(t)+y(t)](\alpha) &= \bigvee_t x(t)+y(t)-\alpha t \\ &\le \bigvee_t y(t) + \bigwedge_b X(b) + bt - \alpha t \\ &\le \bigwedge_b X(b) + \bigvee_t y(t) - (\alpha - b)t \\ &= \bigwedge_b X(b) + Y(\alpha - b). \end{aligned} \tag{61}$$

The first inequality follows from (28), and the second is true because for any real-valued function $f(a,b)$, we have $\bigvee_a \bigwedge_b f(a,b) \le \bigwedge_b \bigvee_a f(a,b)$.

Now, if y is convex, then $y(t) = \bigvee_\alpha Y_\wedge(\alpha) + \alpha t$. Hence

$$\begin{aligned}\mathcal{A}_\vee[x(t)+y(t)](\alpha) &= \bigvee_t x(t) + \bigvee_b Y_\wedge(b) + bt - \alpha t \\ &= \bigvee_b Y_\wedge(b) + X_\vee(\alpha - b) \\ &= X_\vee(\alpha) \oplus Y_\wedge(\alpha). \end{aligned} \tag{62}$$

Thus, under the constraint that one of the signals is convex, adding two signals in time corresponds to dilating or eroding their slope transforms. Note the analogy with LTI systems, where multiplying two signals in time corresponds to convolving their Fourier transforms.

Time-Limiting: Consider a signal $x(t)$ added with a symmetric rectangular time pulse $w(t)$ equal to $w(t) = 0$ for $|t| \le T$ and $-\infty$ elsewhere. This addition time-limits $x(t)$ over the interval $[-T, T]$. The time-limited signal is

$$x_T(t) = \begin{cases} x(t), & |t| \le T \\ -\infty, & |t| > T. \end{cases} \tag{63}$$

Assuming $x(t)$ is concave, the upper slope transform $X_T(\alpha)$ of $x_T(t)$ is

$$X_T(\alpha) = \bigvee_{|t|\le T} x(t) - \alpha t \tag{64}$$

$$= \bigvee_{|t|\le T} \bigwedge_b X(b) + (b-\alpha)t \tag{65}$$

$$= \bigwedge_b X(b) + |b-\alpha|T \tag{66}$$

where the transition from (65) to (66) is possible because $X(b)$ and $X(b)+(b-\alpha)t$ are convex functions of b. The last result establishes that

$$\mathcal{A}_\vee[x_T(t)] = X(\alpha) \ominus (-T|\alpha|) = X(\alpha) \square T|\alpha|. \tag{67}$$

This result is also valid when $x(t)$ is not concave, assuming that $x(t) < +\infty$ for all t, because then $X(\alpha)$ uniquely corresponds to the upper envelope $\hat{x}(t)$, and time-limiting $x(t)$ also time-limits $\hat{x}(t)$. Thus, time-limiting a signal over the interval $[-T, T]$ erodes its upper slope transform by the conical structuring element $-T|\alpha|$. As shown in Fig. 5, this results into replacing high-slope parts of the original slope transform with two supporting tangent lines of slope $\pm T$. These high-slope parts will be the semi-infinite slope intervals where $\alpha > \hat{x}'(-T)$ and $\alpha < \hat{x}'(T)$.

Signal Opening: Let $x(t)$ be a concave and (without loss of generality) even signal. Consider its opening

$$y(t) = [x(t) \ominus g(t)] \oplus g(t) \tag{68}$$

by a flat structuring element $g(t) = 0$ for $|t| \le T$ and $-\infty$ else. As shown in Fig. 6, such a flat morphological opening cuts off the signal peaks whose support has length smaller than

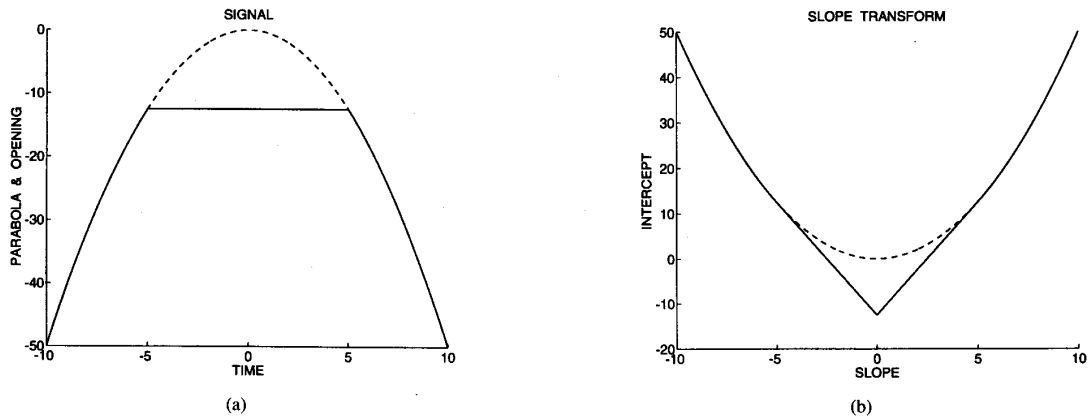

(a) (b)

Fig. 6. (a) Original parabola signal $x(t) = -t^2/2$ (in dashed line) and its morphological opening (in solid line) by a flat structuring element $[-5, 5]$. (b) Upper slope transform of the parabola (in dashed line) and of its opening (in solid line).

$2T$. The effect in the slope domain is to replace the low-slope parts of the original transform with supporting tangent lines. Specifically, the upper slope transform of the opening is

$$Y_\vee(\alpha) = \begin{cases} T|\alpha| + x(T), & |\alpha| \le \alpha_T \\ X(\alpha), & |\alpha| \ge \alpha_T \end{cases} \tag{69}$$

where the breakpoint is at the slope $\alpha_T = |x'(T)|$. Likewise, the *closing* of a convex signal will replace the low-slope parts of its lower slope transform with lines. Finally, if x is a general signal, then the above effects apply to its concave/convex segments.

Duality Between Time and Slope Domain: If we sequentially apply to any signal $x(t)$ the upper slope transform followed by the lower slope transform, we return to the time domain

$$x(t) \overset{\mathcal{A}_\vee}{\longmapsto} X_\wedge \overset{\mathcal{A}_\wedge}{\longmapsto} \hat{x}(-t). \tag{70}$$

Of course, if x is concave, and hence, $x = \hat{x}$, then $\mathcal{A}_\wedge[\mathcal{A}_\vee[x(t)] = x(-t)$. This duality between time and slope domains implies that, for any mapping between a time function to a slope function, there also exists its dual mapping where the role of the two functions is interchanged. For example, time lines become slope impulses and vice-versa; also, time cones become slope pulses, and time pulses become slope cones.

As Table II shows, the lower slope transform has very similar properties with the upper transform, the only differences being the interchange of suprema with infima and dilation with erosion.

In [4], several properties of the stationary-point-based Legendre transform (41) were given that seem similar to the properties of the upper slope transform, but there are some important differences. First, the stationary-point-based transform is generally multivalued, and hence, adding lines to or shifting and scaling of this transform has to be understood as a simultaneous vector translation or homothetic scaling of a set. Second, and most important, the dilation–addition property (60) of the upper slope transform must undergo two significant changes in order to retain a similar form for the multivalued Legendre transform: 1) The supremum in the morphological signal dilation is replaced by values at stationary points (and hence, it becomes set-valued), and 2) the addition of transforms becomes a Minkowski set addition.

TABLE II
PROPERTIES OF LOWER SLOPE TRANSFORM

Signal	Transform
$x(t)$	$X(\alpha) = \bigwedge_t x(t) - \alpha t$
$\bigwedge_i c_i + x_i(t)$	$\bigwedge_i c_i + X_i(\alpha)$
$x(t - t_0)$	$X(\alpha) - \alpha t_0$
$x(t) + \alpha_0 t$	$X(\alpha - \alpha_0)$
$x(rt)$	$X(\alpha/r)$
$x(-t)$	$X(-\alpha)$
$x(t) = x(-t)$	$X(\alpha) = X(-\alpha)$
$rx(t)$, $r > 0$	$rX(\alpha/r)$
$x(t) \square y(t)$	$X(\alpha) + Y(\alpha)$
$\bigwedge_\tau x(\tau) + y(t + \tau)$	$X(-\alpha) + Y(\alpha)$
$x(t) \le y(t)\ \forall t$	$X(\alpha) \le Y(\alpha)\ \forall \alpha$
$\bigwedge_t x(t) = X(0)$	$\bigvee_\alpha X(\alpha) \le x(0)$
$x(t) \vee y(t)$	$\ge X(\alpha) \vee Y(\alpha)$
$x(t) + y(t)$	$\ge X(\alpha) + Y(\alpha)$
$x(t) + y(t)$, y is concave	$X_\wedge(\alpha) \square Y_\vee(\alpha)$
$y(t) = \begin{cases} x(t), & \lvert t\rvert \le T \\ +\infty, & \lvert t\rvert > T \end{cases}$	$Y(\alpha) = X(\alpha) \oplus (-T\lvert\alpha\rvert)$

VI. SLOPE-SELECTIVE FILTERS

One of the most useful applications of LTI systems is the design of frequency-selective filters, e.g., approximations to an ideal lowpass filter with frequency response $H(\omega)$ equal to one for $|\omega| \le \omega_0$ and zero else. We show next that it is also possible to design morphological systems that have a slope selectivity and can be used for envelope estimation.

Imagine a DTI system that rejects all line components with slopes in the band $[\alpha_1, \alpha_2]$ and passes all the rest unchanged. Then its slope response would be

$$G(\alpha) = \begin{cases} 0, & \alpha_1 \le \alpha \le \alpha_2 \\ +\infty, & \text{else.} \end{cases} \tag{71}$$

This is a general ideal-cutoff *slope bandpass* filter. In the time domain, it acts as a morphological dilation by its impulse

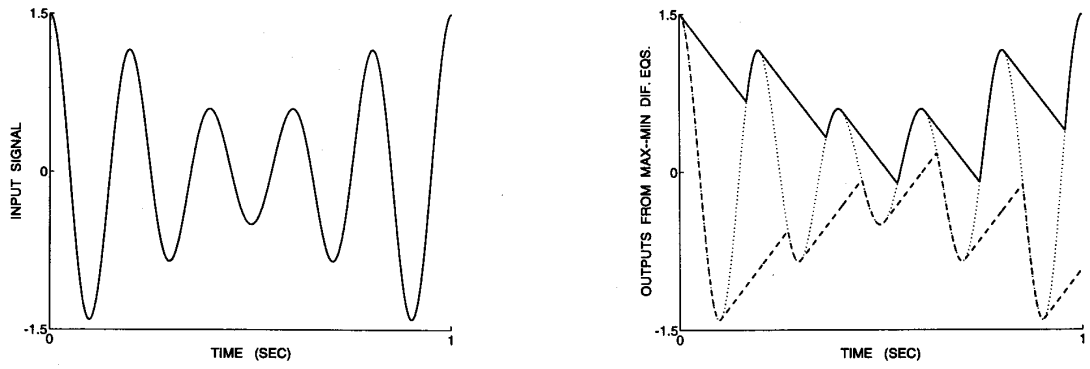

Fig. 7. (a) Original signal $x(t) = [1 + 0.5 \cos (2\pi t)] \cos (10\pi t)$. (b) Upper solid line is the output of a max differential equation with coefficient $\alpha_0 = -5$ whose input is the signal $x(t)$. Lower dashed line is the output of the corresponding min differential equation.

response (found via $\bigwedge_\alpha G(\alpha) + \alpha t$)

$$g(t) = \begin{cases} \alpha_1 t, & t \geq 0 \\ \alpha_2 t, & t \leq 0 \end{cases} \tag{72}$$

which is a concave cone. However, this is not a causal dilation, and hence, it is not realizable. But if we view $g = g_1 \vee g_2$ as the maximum of two signals

$$g_1(t) = \alpha_1 t + \lambda(t), \quad g_2(t) = \alpha_2 t + \lambda(-t) \tag{73}$$

one causal and the other anticausal, then we could implement the dilation by g, by

- dilating the input $x(t)$ by the causal $g_1(t)$ and producing an output $y_1(t) = x(t) \oplus g_1(t)$.
- dilating the input $x(t)$ by the anticausal $g_2(t)$; this can be implemented by reversing time, dilating $x(-t)$ by $g_2(-t)$, and reversing time again to produce $y_2(t) = x(t) \oplus g_2(t)$.
- taking the maximum of the two outputs.

For simplicity, assume now that $\alpha_2 = -\alpha_1 = \alpha_0 > 0$, which makes G a symmetric bandpass filter rejecting all slopes with $|\alpha| > \alpha_0$ and g a symmetric cone. Fig. 7 shows an example of running a signal $x(t)$ through a dilation by the half-line $g_1(t) = -\alpha_0 t + \lambda(t)$. It produces a type of upper envelope where, scanning toward the positive time direction, all the parts of the signal with slope larger than $-\alpha_0$ remain unchanged, whereas parts with slope smaller than $-\alpha_0$ are covered by lines of slope $-\alpha_0$ that extend until points of the signal graph with slope larger than $-\alpha_0$. After such points, the same pattern repeats. The dynamics of this causal dilation $x(t) \mapsto y(t) = x(t) \oplus g_1(t)$ are described by the following first-order nonlinear differential equation:

$$\begin{aligned} y(0) &= x(0) \\ y'(t+) &= \begin{cases} \max(x'(t+), -\alpha_0), & \text{if } y(t) = x(t) \\ -\alpha_0, & \text{if } y(t) > x(t) \end{cases} \end{aligned} \tag{74}$$

where $x'(t+) = \lim_{p \downarrow 0} [x(t+p) - x(t)]/p$. The reason for using right-sided derivatives is twofold: i) they are sufficient to create the forward dynamics, and ii) the input and the output signals are assumed continuous, but they might not possess a two-sided derivative at all points.

Consider now a system $x(t) \mapsto y(t)$ described by the first-order linear differential equation $y'(t) + ay(t) = x(t)$. Assuming zero initial conditions and the system being initially at rest, this corresponds to an LTI system whose impulse response is a causal exponential $h(t) = \exp(-at), t \geq 0$ and its frequency response $H(\omega) = 1/(a + j\omega)$ has magnitude $1/\sqrt{a^2 + \omega^2}$. Thus, although both the above linear and nonlinear differential equations are of first order, and they correspond to systems whose impulse responses h and g are eigenfunctions of LTI and DTI systems, respectively, the frequency response of the LTI system is only approximately lowpass, whereas the slope response of the DTI system has an ideal cut-off characteristic. Further, this ideal analog slope filter is realizable in the time domain either via a dilation with a causal line or via running the dynamical system of (74). This analog slope filter described by (74) can be hardware-implemented with electronic circuits using analog differentiators and comparators.

Whatever we discussed for DTI systems extends to ETI systems, too, with only a few minor changes. An ETI system with slope response

$$F(\alpha) = \begin{cases} 0, & \alpha_1 \leq \alpha \leq \alpha_2 \\ -\infty, & \text{else} \end{cases} \tag{75}$$

acts as an ideal slope bandpass filter with impulse response

$$f(t) = \begin{cases} \alpha_2 t, & t \geq 0 \\ \alpha_1 t, & t \leq 0 \end{cases} \tag{76}$$

which is a convex cone. The bandpass DTI and ETI systems are closely related because $F(\alpha) = -G(\alpha)$ and $f(t) = -g(-t)$. Their difference is that the DTI system yields as output an upper envelope of the input signal, whereas the ETI system produces a lower envelope. As for the DTI system, the above ETI system can be realized by taking the minimum of the outputs of two ETI systems, one with causal impulse response $\alpha_2 t - \lambda(t)$ and the other with anticausal impulse response $\alpha_1 t - \lambda(-t)$. Each system can be realized in the time domain either by eroding the input by a half-line or by running a dynamical system based on a minimum version of the differential equation in (74). If $\alpha_2 = -\alpha_1 = \alpha_0 > 0$, then

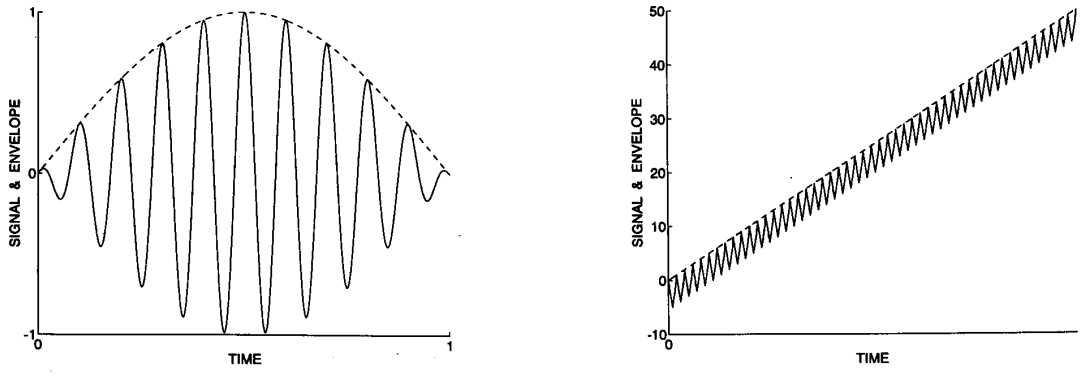

Fig. 8. Signals x (in solid lines) and their upper envelopes $\hat{x}$ (in dashed lines) obtained via the composition of the upper slope transform and its inverse. Signals are (a) a cosine whose amplitude has been modulated by a slower cosine pulse and (b) the output x of a recursive discrete DTI system described by the max difference equation $x[n] = \max(u[n], \bigvee_{1 \le k \le 10} x[n-k] + a_k)$, where $a_k = -|5-k|$ for $k = 1, \cdots, 9$, $a_{10} = 1$, and the input is $u[n] = \mu[n]$.

this differential equation for the causal ETI system is

$$y'(t+) = \begin{cases} \min(x'(t+), \alpha_0), & \text{if } y(t) = x(t) \\ \alpha_0, & \text{if } y(t) < x(t) \end{cases} \tag{77}$$

with $y(0) = x(0)$. The output of this dynamical system is shown in Fig. 7(b) as the lower envelope.

VII. Discussion

We conclude with some general comments on slope transforms and some of their extensions.

A. Concluding Remarks on Slope Transforms

An arbitrary signal can be analyzed using slope transforms in at least two different ways corresponding to two different goals: signal reconstruction or envelope reconstruction. If the goal is exact signal reconstruction, then we should first segment the signal into consecutive convex and concave pieces. If the signal x is twice differentiable, this can be done by finding the inflection points $x'' = 0$, where we have transitions between convexity and concavity. Then we find the slope transform of each piece, either using Legendre transform if it is a known and differentiable mathematical function or using the upper/lower slope transforms for general signals. The result will generally be a set collection of slope transforms of the signal pieces, which can reconstruct the signal exactly. The disadvantage here is the multivaluedness of the transform. Alternatively, if the analysis goal is more to extract information about the long-term behavior of the signal, as manifested by its upper and lower envelope, then we could compute its upper and lower slope transform and take their inverses. As Fig. 8 shows, if the signal has the form of a wavelet packet with tapered ends and some type of oscillations between an upper and a lower envelope, then the inverse upper and lower slope transform can provide us with the useful information of the upper and lower envelope. All the oscillations between the two envelopes are ignored, but they may not be important if our envisioned application is envelope detection, as for instance in AM signals.

The differences between the upper/lower slope transforms and the Legendre transform include the following: i) The sup/inf-based transforms are more general because they can apply to nondifferentiable signals, whereas the Legendre transform cannot. ii) For differentiable signals, the Legendre transform is generally multivalued, whereas the sup/inf-based transforms are single-valued. Of course, the upper/lower slope transforms can be made multivalued by applying them to each individual concave/convex segment of a signal and defining the transform of the total signal as the collection of the individual transforms. iii) The sup/inf-based transforms allow functions defined over the whole slope or time axis by padding time-limited or slope-limited functions with $\pm\infty$ values, but the Legendre transform cannot extend the time or slope functions beyond their domain of definition. iv) For discrete-time signals only the sup/inf-based transforms can directly apply because the Legendre transform requires time derivatives that are not well or uniquely defined for discrete-time signals.

B. Multidimensional Signals

Consider a d-dimensional signal $x : \boldsymbol{R}^d \to \overline{\boldsymbol{R}}$ with $d = 2, 3, \cdots$. We define its upper slope transform as

$$X_\vee(\vec{\alpha}) \triangleq \bigvee_{v_1 \in \boldsymbol{R}} \cdots \bigvee_{v_d \in \boldsymbol{R}} x(\vec{v}) - \langle \vec{\alpha}, \vec{v} \rangle \tag{78}$$

where $\vec{v} = (v_1, \cdots, v_d)$ is the position vector, $\vec{\alpha} = (\alpha_1, \cdots, \alpha_d) \in \boldsymbol{R}^d$ is the slope vector, and $\langle \vec{\alpha}, \vec{v} \rangle = \Sigma_{i=1}^d \alpha_i v_i$ denotes inner product. The inverse upper slope transform of $X_\vee$ is the signal

$$\hat{x}(\vec{v}) \triangleq \bigwedge_{\alpha_1 \in \boldsymbol{R}} \cdots \bigwedge_{\alpha_d \in \boldsymbol{R}} X_\vee(\vec{\alpha}) + \langle \vec{\alpha}, \vec{v} \rangle \tag{79}$$

which is the smallest concave upper envelope of x. The properties of this multidimensional transform are very similar to and can be easily inferred from the 1-D case.

Consider now a multidimensional DTI system $\mathcal{D} : x(\vec{v}) \mapsto y(\vec{v})$. The signals $x(\vec{v}) = \langle \vec{\alpha}, \vec{v} \rangle + b$ are eigenfunctions of $\mathcal{D}$

because the corresponding outputs are $y(\vec{v}) = \langle \vec{\alpha}, \vec{v} \rangle + b + G(\vec{\alpha})$ with

$$G(\vec{\alpha}) \triangleq \bigvee_{\vec{v}} g(\vec{v}) - \langle \vec{\alpha}, \vec{v} \rangle$$

where $g = \mathcal{D}(\mu)$ and $\mu(\vec{v}) = \Sigma_i \mu(v_i)$.

For 2-D signals $g(v_1, v_2), G(\alpha_1, \alpha_2)$ has two slope variables: horizontal and vertical. Next, we give a few examples of the slope responses of DTI systems whose impulse responses are structuring functions often used in morphological image processing.

Example 11: Sphere/disk: Consider a spherical structuring function ($A \geq 0$)

$$g(v_1, v_2) = \begin{cases} A\sqrt{1 - v_1^2 - v_2^2}, & v_1^2 + v_2^2 \leq 1 \\ -\infty, & \text{else.} \end{cases} \quad (80)$$

Since g is concave and has an invertible gradient, its upper slope transform G is equal to its 2-D Legendre transform, which can be found via stationary points. Namely, setting $\partial g / \partial v_i = \alpha_i$ for $i = 1, 2$ and finding the value of $g(\vec{v}^*) - \langle \vec{\alpha}, \vec{v}^* \rangle$ at $\vec{v}^* = (\nabla g)^{-1}(\vec{\alpha})$ yields

$$G(\alpha_1, \alpha_2) = \sqrt{A^2 + \alpha_1^2 + \alpha_2^2}. \quad (81)$$

By taking the limit of as $A \to 0, g$ becomes a flat disk with radius one, and the slope response G becomes $\sqrt{\alpha_1^2 + \alpha_2^2}$.

Example 12: Rectangle: Consider a flat rectangular structuring function

$$g(v_1, v_2) = \begin{cases} 0, & |v_1| \leq T_1 \text{ or } |v_2| \leq T_2 \\ -\infty, & \text{else.} \end{cases} \quad (82)$$

The gradient of g is not invertible, and hence, we cannot use the stationary points approach. Instead, we directly find the supremum of $g(\vec{v}) - \langle \vec{\alpha}, \vec{v} \rangle$, i.e.

$$\begin{aligned} G(\alpha_1, \alpha_2) &= \bigvee_{|v_1| \leq T_1} \bigvee_{|v_2| \leq T_2} -(\alpha_1 v_1 + \alpha_2 v_2) \\ &= T_1 |\alpha_1| + T_2 |\alpha_2|. \end{aligned} \quad (83)$$

Example 13: Paraboloid: The 2-D parabola

$$g(v_1, v_2) = -0.5(v_1^2 + v_2^2) \quad (84)$$

has invertible gradient $\nabla g = -\vec{v}$. Hence, setting $\nabla g(\vec{v}^*) = \vec{\alpha}$ and finding the value of $g(\vec{v}^*) - \langle \vec{\alpha}, \vec{v}^* \rangle$ yields the upper slope (and Legendre) transform G

$$G(\alpha_1, \alpha_2) = 0.5(\alpha_1^2 + \alpha_2^2). \quad (85)$$

If we see all the above concave symmetric functions g as structuring elements for dilations, then these DTI systems have a convex symmetric slope response G. Since a relatively high value of $G(\alpha)$ implies that input lines αt are deemphasized in the output, the convexity and symmetry of G make it approximately a lowpass slope response.

C. Discrete-Time Signals

Let $x_c(t)$ be a continuous-time signal, and let $X_c(\alpha) = \bigvee_t x_c(t) - \alpha t$ be its upper slope transform. Consider *sampling* $x_c(t)$ at time instants $t = nT$ that are integer multiples of a sampling period T. For applying slope transforms, we model the sampling as addition of the original signal with a periodic morphological impulse train $p(t) = \bigvee_n \mu(t - nT)$. Thus, the sampled signal is

$$x_s(t) = x_c(t) + p(t) = \bigvee_n x[n] + \mu(t - nT) \quad (86)$$

where $x[n] = x_c(nT), n = 0, \pm 1, \pm 2, \cdots$ is the discrete-time signal. Then the upper slope transform of the sampled signal is

$$X_s(\alpha) = \bigvee_n x[n] - \alpha n T. \quad (87)$$

Since the supremum is only over discrete time instants, we have $X_s(\alpha) \leq X_c(\alpha)$. Thus, sampling generally decreases the values of the upper slope transform. Equality at any α, i.e., $X_s(\alpha) = X_c(\alpha)$, occurs if the time t^* at which x_c has slope α is a sampling instant, i.e., if $t^* = (x_c')^{-1}(\alpha) = nT$ for some n.

Further, $X_s(\alpha)$ is always a convex piecewise-linear function. Thus, if $x_c(t)$ is a concave piecewise-linear signal and the sampling time instants $t = nT$ include all the times at which its corner points occur, then (see example 5) $X_c(\alpha) = X_s(\alpha)$ for all α, and the original signal $x_c(t)$ can be exactly reconstructed from its samples by applying an upper slope transform on $x_s(t)$ followed by its inverse transform.

Now, if we define the upper slope transform of the discrete-time signal $x[n]$ by

$$X_d(\alpha) \triangleq \bigvee_n x[n] - \alpha n \quad (88)$$

we have that

$$X_d(\alpha) = X_s(\alpha / T) \leq X_c(\alpha / T). \quad (89)$$

Namely, the slope transform of the discrete-time signal is a slope-scaled version of the transform of the continuous-time sampled signal.

Very similar results can be obtained for the relationship between the continuous- and discrete-time lower slope transform; the latter is defined as in (88) by replacing supremum with infimum.

With the exception of the time scaling property $x(rt) \leftrightarrow X(\alpha / r)$, the properties of the discrete-time (upper or lower) slope transform are identical to its continuous-time counterpart. Further, as the slope transforms proved to be useful analytic tools for continuous-time morphological systems, their discrete-time counterparts also greatly aid the analysis of discrete DTI or ETI systems, especially of the recursive type; examples are given in [7].

ACKNOWLEDGMENT

The author wishes to thank Henk Heijmans for bringing to his attention references [1], [9], and [5] and for useful comments.

REFERENCES

[1] R. Bellman and W. Karush, "On the maximum transform," *J. Math. Anal. Appl.*, vol. 6, pp. 67–74, 1963.

[2] H. B. Callen, *Thermodynamics and an Introduction to Thermostatistics*. New York: Wiley, 1985.

[3] R. Courant and D. Hilbert, *Methods of Mathematical Physics*. New York: Wiley, 1962.

[4] L. Dorst and R. van den Boomgaard, "An analytical theory of mathematical morphology," in *Proc. First Int. Workshop Math. Morphol. Applicat. Signal Processing*, Barcelona, Spain, May 1993.

[5] P. K. Ghosh, "An algebra of polygons through the notion of negative shapes," *CVGIP: Image Understanding*, vol. 54, no. 1, pp. 119–144, 1991.

[6] H. J. A. M. Heijmans, *Morphological Image Operators*. Boston, MA: Academic, 1994.

[7] P. Maragos, "Max-min difference equations and recursive morphological systems," in *Proc. First Int. Workshop Math. Morphol. Applicat. Signal Processing*, Barcelona, Spain, May 1993.

[8] P. Maragos and R. W. Schafer, "Morphological systems for multidimensional signal processing," *Proc. IEEE*, vol. 78, pp. 690–710, Apr. 1990.

[9] R. T. Rockafellar, *Convex Analysis*. Princeton: Princeton Univ. Press, 1972.

[10] J. Serra, *Image Analysis and Mathematical Morphology*. New York: Academic, 1982.

[11] ——, *Image Analysis and Mathematical Morphology, Vol. 2: Theoretical Advances*. New York: Academic, 1988.

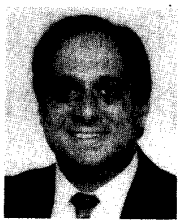

Petros Maragos (S'81–M'85–SM'91) received the Diploma degree in electrical engineering from the National Technical University of Athens, Greece, in 1980 and the M.S.E.E. and Ph.D. degrees from the Georgia Institute of Technology, Atlanta, in 1982 and 1985, respectively.

In 1985, he joined the faculty of the Division of Applied Sciences at Harvard University, where he worked as Assistant (1985–1989) and Associate Professor (1989–1993) of Electrical Engineering. During the fall of 1992, he was a Visiting Professor at the National Technical University of Athens. In 1993, he joined the faculty at Georgia Institute of Technology, where he is currently an Associate Professor of Electrical and Computer Engineering. He has been a consultant to Xerox's research on document image processing and to the Greek Institute for Language and Speech Processing in Athens. His research and teaching activities have been in the general areas of signal processing, systems theory, communications, and applied mathematics and their applications to image processing and computer vision and computer speech processing and recognition.

In 1987, Dr. Maragos received a National Science Foundation Presidential Young Investigator Award for his work in signal and image processing. He is the recipient of the 1988 IEEE Acoustics, Speech, and Signal Processing Society's Paper Award for the paper "Morphological Filters." He is also the co-recipient of the 1994 IEEE Signal Processing Society's Senior Award and co-recipient of the 1995 IEEE Baker Prize Award, both for the paper "Energy Separation in Signal Modulations with Application to Speech Analysis." His professional society activities include Associate Editor and Guest Editor for the IEEE TRANSACTIONS ON SIGNAL PROCESSING and IEEE TRANSACTIONS ON IMAGE PROCESSING, General Chairman for the 1992 SPIE Conference on Visual Communications and Image Processing, member of the IEEE DSP and IMDSP Technical Committees, and President of the International Society of Mathematical Morphology.